# Stratigraphic analysis of a sediment pond within the New England Mud Patch: New constraints from high-resolution chirp acoustic reflection data

John A. Goff[1], Jason Chaytor[2], Allen H. Reed[3], Glen Gawarkiewicz[4], Preston S. Wilson[5], and David P. Knobles[6]

[1]*Institute for Geophysics, Jackson School of Geosciences, University of Texas at Austin*

[2]*USGS Woods Hole*

[3] Minewarfare and Databasing, *NAVOCEANO, 1002 Balch Blvd, Stennis Space Center, MS 39522*

[4]*Woods Hole Oceanographic Institution*

[5]*University of Texas at Austin Department of Mechanical Engineering and Applied Research Laboratories*

[6]*KSA, LLC*

Submitted to *Marine Geology*, September, 2018

**Abstract**

The New England Mud Patch is an anomaly on the Atlantic coast of North America. This ~13,000 $km^2$ area, located south of Cape Cod between the ~60 m and 160 m isobaths, is a region of active fine-grained deposition on a shelf that is predominantly non-depositional or erosional. Prior studies theorized that Mud Patch sediments are derived from fines winnowed from Georges Bank, transported westward by coastal currents, and then settled in more quiescent conditions at the Mud Patch. A chirp seismic reflection (2015) and coring (2016) survey of the Mud Patch was conducted in support of a planned acoustic experiment for the Office of Naval Research. The survey focused on a ~30 km (E-W) by ~8 km (N-S) region between the 75 m and 85 m isobaths, encompassing a sediment "pond" >12 m thick. The dense (250 m) survey lines allow a pseudo-3D stratigraphic interpretation. The sediment pond itself occupies an accommodation space that appears to have been eroded into substrate (Pleistocene?) sediments, perhaps by glacial outwash. The interpreted transgressive ravinement is capped by marine sands organized into oblique sand ridge morphology. The sense of obliquity, morphologic asymmetry, and internal dipping reflectors indicate that the sand ridges formed under an east-directed transport regime. However, as evidenced by prograding internal layering, Mud Patch deposition occurred under a west-directed transport regime, consistent with modern shelf conditions. The onset of fine-grained deposition was therefore contemporaneous with a significant shift in the hydrologic regime. Muds deposited above the transitions include a significant sand component, whose modal grain size is identical to the sand beneath the transition. This admixture could be explained by the fact that, during the early stages of Mud Patch deposition, the tops of the sand ridges remained exposed. Episodic, storm-driven transport of sand to the muddy deposits may account for the internal layering of the Mud Patch.

Key Words: New England shelf, mud patch, sand ridges, chirp, vibracore

## 1. Introduction

The continental shelf of the Mid Atlantic Bight, from Cape Hatteras to Cape Cod, is predominantly a non-depositional environment (Emery and Uchupi, 1972), with a seafloor dominated by medium to coarse sands (Fig. 1). The seabed is largely organized into oblique sand ridges that first developed on the shoreface and inner shelf, and later were stranded in deeper water by sea level rise and the transgressed shoreline (Swift et al., 1973; Swift and Field, 1981; Goff et al., 1999). The scarcity of terrigenous sedimentary input onto the shelf (Milliman et al., 1972) and storm-dominated hydraulic regime (Butman et al., 1979; Swift et al., 1981; Vincent et al., 1981) combine to keep the shelf sand ridges exposed and active at the seafloor, uncovered by subsequent fine-grained marine deposition (Duane et al., 1972; Goff et al., 2005; Snedden et al., 2011). There are, however, important exceptions to this general characterization. The Hudson Shelf Valley, for example (Fig. 1), is a locus of modern fine-grained deposition, owing in large part to the still-present accommodation space in relation to the surrounding seafloor (Freeland et al., 1981; Vincent et al., 1981). But by far the most significant region of fine-grained deposits on the Mid-Atlantic Bight continental shelf is the southern New England "Mud Patch" (Milliman et al., 1972; Twichell et al., 1981; Bothner et al., 1981), a wide (~13,000 $km^2$) region of silty/muddy sediments south of Cape Cod (Fig. 1). The presence of this large anomaly makes it an important topic of study for helping to understand marine depositional processes on the continental shelf.

Early speculation regarding the origin of the Mud Patch was split between relict or modern deposit. Garrison and McMaster (1966) suggested that the muds overlie basal transgressive sands that emerge to the north and west, but are in turn overlain by Nantucket Shoals sand to the east; this would imply a relict (though recent) deposit, which was earlier suggested by Shepard and Cohee (1936) and Uchupi (1963), and later by Ross (1970) and Schlee (1973). Stetson (1938), however, asserted that these sediments were terrestrial in origin, and modern in age; Emery (1965) also indicated in his sediment

maps that the Mud Patch is a modern deposit. The most recent and comprehensive published survey of the Mud Patch was conducted in 1978 (Twichell et al., 1981; Bothner et al., 1981), consisting of 1450 km of shallow subbottom profiles (mostly Huntec seismic data), 1220 km of sidescan sonar, and 7 vibracores up to 6 m in length. The mud unit was observed to be acoustically transparent and up to ~12 m thick in locations (Twichell et al., 1981). Beneath the mud, Twichell et al. (1981) observed an undulating morphology and postulated, similarly to Garrison and McMaster (1966), that it was relict ridge-and-swale features formed in the transgressive sands, then buried by mud as sea level rose during the Holocene. However, no evidence was found that Nantucket Shoals sands overlay the muds, as Garrison and McMaster (1966) also suggested. Sidescan reveal the Mud Patch seafloor to be largely featureless, except for trawl marks, but with evidence for recent storm-driven mobility of sediments based on tripod-based bottom photography (Twichell et al., 1981). Geochemical analyses of core samples (Bothner et al., 1981) indicated modern mud accumulation, and that depositional rates have waned over time from 130 cm/1000 y near the beginning of deposition to 25 cm/1000 y today. Twichell et al. (1981) hypothesized that Georges Bank and Nantucket Shoals to the east are the source of the fine-grained sediments of the Mud Patch; storms and strong tidal currents could be winnowing/eroding the available fine-grained material, and west-directed shelf currents could transport it. In the vicinity of the Mud Patch, the tidal currents are weaker (away from the tidal resonance in the Gulf of Maine), allowing for fine-grained sediment deposition (Shearman and Lentz, 2004). Twichell et al. (1981) further suggested that the waning accumulation rates reported by Bothner et al. (1981) could be explained by a decrease in supply of winnowed material over time. The Twichell et al. (1981) interpretation was, however, called into question by Mazzula et al. (1988) who, in a study of coarse silt distribution in the Mid-Atlantic Bight, found an abundance of glacial silt on Georges Bank and Nantucket Shoals but a dearth of such sediments within the Mud Patch. They infer that Mud Patch silts were likely sourced from coastal plain

83 strata and the Appalachians of New England eroded during Last Glacial Maximum (LGM). The origin of
84 the New England Mud Patch, and the reason for its existence, therefore remains enigmatic.

85 Several decades of advances in geophysical survey technology, interpretation software, and core
86 analysis make the Mud Patch region appropriate for further study. In addition, the installation of the
87 Pioneer Array (part of the Ocean Observatory Initiative; http://www.whoi.edu/ooi_cgsn/pioneer-array)
88 at the seaward edge of the Mud Patch, has prompted renewed interest in understanding the
89 oceanographic and sedimentary processes in the region (Chen et al., 2018; Gawarkiewicz et al., 2018). In
90 an effort to initiate such an investigation, reconnaissance chirp acoustic reflection data were collected in
91 2012 aboard the *R/V Tioga* (funded as a seed grant by the University of Texas Jackson School of
92 Geoscience). Survey lines crossed some of the thickest portions of the Mud Patch, including a ~12-m
93 deep sediment pond earlier identified by Twichell et al. (1981). These data reveal that, far from being a
94 transparent unit, the seismic facies of the Mud Patch unit is highly laminated, with increasing reflectivity
95 at increasing depth (Fig. 2). The data also reveal evidence of onlap and ponding on the undulating basal
96 surface interpreted by Twichell et al. (1981) as relict sand ridges, as well as a deeper reflector that
97 appears to form a basal reflector for these features (Fig. 2). These reconnaissance observations
98 demonstrate that a detailed stratigraphic history of the Mud Patch is accessible to a comprehensive
99 chirp survey.

100 Such a survey was eventually conducted in 2015 as part of the Office of Naval Research-sponsored
101 Seabed Characterization Experiment (SCE) (Wilson and Knobles, 2017; Wilson and Knobles, in
102 preparation). The goals of SCE centered around measuring and modeling acoustic interactions with a
103 fine-grained seabed and the ability to infer sediment properties via remote sensing in a continental shelf
104 setting; the presence of the Pioneer Array, proximity to ships, ports and facilities, as well as the excellent
105 record provided by the reconnaissance chirp data (Fig. 2) made the Mud Patch a strong candidate for
106 the experiment location. Environmental characterization was provided by geophysical survey and core

collection in 2015 and 2016, and a multi-ship acoustic experiment was conducted in 2017. The experiment was focused in particular on the aforementioned sediment pond (Fig. 2), both because of its greater thickness of fine-grained sediments, and because of its fortuitous location between two major shipping lanes made it free of significant ship traffic. In this paper we report primarily on the stratigraphic analysis of the chirp acoustic reflection data (Fig. 1, inset) over the sediment pond. We will also present photographic and grain size analysis of one core to examine the nature of the sand-to-mud transition at the base of the Mud Patch unit.

## 2. Methods

### 2.1 Chirp Acoustic Reflection

The SCE subbottom reflection survey was conducted aboard the *R/V Sharp* in July of 2015, within a box region ~30 km long in the E-W direction and ~11 km wide in the N-S direction (Fig. 1, inset). The survey consisted of 42 E-W (strike) lines with a spacing of ~250 m, crossed by 6 N-S (dip) and two diagonals as well as two of the 2012 reconnaissance chirp lines (Fig. 1, inset); another reconnaissance line was situated just west of the survey box. These data were collected with an Edgetech 512 chirp system operating primarily with a 0.5-7.2 kHz, 30 ms pulse. Two sets of chirp records are preserved and processed: (1) the full-waveform output of the chirp match filter, and (2) a fit of a positive-definite envelope over the top of the sinusoidal full-waveform records (or, simply, the “envelope”). Full-waveform records (e.g., Fig. 2) are most useful for observing smaller-scale details of the subbottom structures, whereas the envelope records are often better for observing large-scale stratigraphy (see further discussion in Goff et al., 2015). Towfish depth was recorded with a self-contained pressure sensor, time-synched to the chirp acquisition computer; these data were used to correct for towfish depth. Towfish heave was also filtered after automated bottom detection. Navigation was recorded

with a differential GPS system using an antenna mounted at the stern of the ship, and a layback correction was estimated trigonometrically by line-out and towfish depth beneath the A-frame tow point. A secondary deconvolution was applied to the full-waveform data; in our experience, the system's match filter does not provide a completely satisfactory result, and image clarity can be significantly improved with this additional processing step (Goff et al., 2015).

Processed full-waveform and envelope records were imported into Landmark DecisionSpace software for interpretation of seismic reflectors. After the seafloor reflection was picked, a cross-tie correction was applied globally using the DecisionSpace tool for that purpose; cross-tie correction, which globally adjusts vertical references on each line to match seafloor arrivals at crossing points, is an effective empirical means of applying a tidal correction without knowing the tides *a priori*. After subsequent interpretation of reflection horizons, results were output in two-way travel time (twtt) and individual horizons were interpolated across the survey regions onto a 0.001° by 0.001° (~0.111 km by 0.085 km) grid. The interpolation was masked over any grid node that was not within 0.2 km of a data point. Isopach grids were formed by subtraction of deeper horizon grids from shallower.

### 2.2 Vibracore

A large suite of vibracores and piston cores were collected in the SCE survey region in 2016 aboard the *R/V Endeavor* by USGS Woods Hole and University of Texas participants. A comprehensive analysis of these core samples will be the topic of a companion publication, but for this study we present an analysis derived from one vibracore that penetrated through the mud-to-sand transition at the base of the Mud Patch in order to illustrate the sedimentary characteristics of this key stratigraphic horizon. Vibracores were collected with a Rossfelder P-3 system, using a buoyancy frame configuration and linerless, 3-inch aluminum barrels. After recovery, barrels were cut into ~1-m sections for logging,

transport and storage. Logging was conducted on board immediately after sectioning using a Geotek multi-sensor core logger (MSCL); measurements included compressional sound speed (at 250 kHz), gamma ray density, resistivity and magnetic susceptibility. Core sections were transported to the USGS Woods Hole core analysis facility, where they were split, photographed, and geologically described. Vibracore subsamples were later collected and analyzed for grain size distribution at the University of Texas at Austin. Histograms of grain sizes were measured using a Malvern Mastersizer 3000 in 0.25$\phi$ bin sizes (where grain size in mm = $2^{-\phi}$). The Mastersizer measures volume fractions using a laser particle diffraction analyzer. Samples were first sieved at 0.85 mm to remain within Mastersizer analysis limits of 1 mm; the portion of material coarser than this aperture (primarily shell hash) was determined by weight and recorded separately from the grain size histogram. Descriptive terms for grain sizes follow the Wentworth (1922) classification.

## 3. Results

### 3.1 Stratigraphic Elements

The overall structure of the mud pond targeted for the SCE is illustrated in Fig. 3, an envelope chirp record spanning the full E-W span of the survey region. The base of the mud unit is clearly identified as a high-amplitude, undulatory reflector, as noted earlier by Twichell et al. (1981). In this cross-section, the shape of the depression that forms the mud pond is asymmetric, with a steeper west flank than east. Laminated reflectors are observed in the interior of the mud pond; several of these onlap on the west flank of the mud pond while draping over the east flank (Fig. 3). The seismic facies of the mud pond transitions upward from laminated to transparent/weakly laminated.

The stratigraphic elements of the survey region can be seen with greater clarity in an enlarged, full-waveform record (Fig. 4). This image focuses on the western flank of the mud pond, where deeper

laminated reflectors onlap the flank of a buried structure of the sort interpreted earlier by Twichell et al. (1981) as a relict sand ridges. The undulatory reflector at the base of the fine-grained sediment (mud) of the Mud Patch is identified as “mb” (mud base; Fig. 4b). Coring (see section 3.4) verifies that this reflector is a mud/sand interface. We have also interpreted five individual reflectors within the laminated mud unit in order to investigate the filling history: “mh1” through “mh5” (Fig. 4b). Another strong reflector (“sb”, or sand base) is observed below “mb”, far less undulatory in character and related to “mb” in that the low points in “mb” merge with “sb” (Figs. 2, 4b). This relationship is identical to that of inner shelf sand ridges with the transgressive ravinement, which serves as a basal surface for the mobile marine sands (e.g., Goff, 2014; Goff et al., 2015). Subtle, east-dipping reflectors can be identified within the ridged feature, between the “sb” and “mb” reflectors (Fig. 4), similar to interior reflections observed in exposed sand ridges on the New Jersey shelf (Goff and Duncan, 2012). Another strong reflector, “db” (deep base), is observed below “sb”, which generally bounds a chaotically reflective seismic facies above from a more transparent facies below (Fig. 4). Although “db” does exhibit topographic variability, over large scales it is generally conformable with the seafloor. Given the stratigraphic relationship to the interpreted transgressive relict sand ridges, the “db” reflector can confidently be interpreted as a pre-transgressive (likely Pleistocene) horizon.

### 3.2 Unit Stratigraphy

A structure map of the “mb” reflection horizon (Fig. 5a) reveals that the mud pond is formed within a topographic embayment. Both within and outside of the embayment, the mud base is floored by a NE-SW trending fabric of ridges and swales spaced ~1-3 km apart. Regional isobaths are oriented ~WNW-ESE in this region, such that the fabric orientation forms an oblique angle of ~65° relative to the contours. The ridge-and-swale morphology is better visualized in the mud unit isopach map (Fig. 5b),

199 which is effectively the mud base structure map detrended by the seafloor. This map also demonstrates
200 that the overall shape of the mud pond is asymmetric, elongated in a ~NW-SE orientation. Maximum
201 thickness measured is ~16 ms twtt, or ~12.8 m (assuming sound speeds in the mud of 1600 m/s for
202 mud), consistent with acoustic measurements made by Twichell et al. (1981) in this area of the Mud
203 Patch.

204 Directly beneath the "mb" horizon, the structure of the ridge-and-swale morphology is also well
205 imaged by the mb-sb isopach map (Fig. 6a), which shows the thickness of these features in relation to
206 their basal horizon. The largest ridges rim the western edges of the mud pond, with thicknesses
207 exceeding 5 ms twtt (~4.5 m assuming sound speed of 1800 m/s for sand). The largest of these ridges
208 also display a pronounced asymmetry (see also Fig. 4), with steeper SE-facing slopes. The ridges are
209 smallest within the base of the mud pond, with peak thicknesses of ~1-2 ms twtt (~0.9-1.8 m), and of
210 intermediate size on the east flank (~2-3 ms twtt, or ~1.8-2.7 m). The obliquity and range in heights and
211 widths of these features are consistent with sand ridges observed elsewhere in the Mid Atlantic Bight
212 (Swift and Field, 1981; Goff et al., 1999).

213 The isopach map for the "sb-db" unit is shown in Fig. 6b; because the "db" horizon is largely
214 conformable with the modern seafloor, this isopach provides a reasonable proxy for the
215 accommodation space available for the ponded sediments. Hence, for example, we observe a strong
216 inverse correlation between the "sb-db" (Fig. 6b) and "seafloor-mb" (Fig. 5b) isopachs. Some of this
217 accommodation space was also filled by the large sand ridges on the western flank of the mud pond (Fig.
218 6a). In the center of this region we have drawn a line that we identify as the "axis of accommodation",
219 which will be used in the following section.

220

### 3.3 Mud Patch Internal Stratigraphy

Isopachs formed from selected internal Mud Patch reflectors can be used to investigate the depositional history of the mud pond (Fig. 7). The earliest sediments deposited in the mud pond ("mh1-mb"; Fig. 7a) preferentially filled in the swales of the underlying morphology, while the ridges along the flanks of the mud pond remained exposed. The depocenter of this unit was to the NE of the axis of accommodation. Shifting forward to the "mh3-mh2" isopach (Fig. 7b), the ridge-and-swale morphology no longer exerts an influence on the depositional pattern in the middle of the pond. However swale-filling does occur around flanks of the pond, ridges to the east now have sediments over their peaks, while the largest ridges to the west were still unsedimented. The depocenter of this unit was centered on the axis of accommodation rather than to the NE. Still later in the stratigraphic sequence ("mh5-mh4"; Fig. 7c), sediments finally cover all of the underlying ridges, and the depocenter shifted again to the SW of the axis of accommodation. The most recent isopach, "seafloor-mh5", is a constant thickness unit throughout the survey region, indicating that the accommodation space for the mud pond was entirely filled at this time.

In summary, the depositional history of the mud pond involved preferential filling of low-lying regions, more rapid transition to draping the eastern flank while still onlapping the western flank (see also Fig. 2), and SW-prograding depocenters.

### 3.4 Core Analysis of Mud/Sand Interface

The mud/sand boundary is a critical transition in the evolution of the Mud Patch. We demonstrate that transition here with a vibracore penetration (core VC2) through the boundary (Figs. 8, 9), using photographic images of split cores, sound speed and density from the Geotek MSCL, and grain size histogram data from core samples; these results are typical of mud/sand transitions cored elsewhere.

Visually, the boundary is observed to have three components: (1) a poorly-sorted sandy mud, (2) a shell-rich layer, and (3) shelly sand (Fig. 8a). Sound speed and density both increase across the boundary (Fig. 8b), averaging ~1580 m/s and ~1840 kg/m$^3$, respectively in the sandy mud, and ~1870 m/s and ~2300 kg/m$^3$, respectively, in the shelly sand. The transition through the shell-rich layer, where coarse fractions change from 0 to 0.29 (Fig. 8), occurs across ~10 cm of core. Median (D50) grain sizes of non-shell sediment likewise shift significantly across the boundary, averaging 18.5 μm in the sandy mud and 347 μm in the shelly sand. The wide dispersion of D10 and D90 grain sizes over most samples indicates very poorly sorted sediments; only the deepest sample in the core can be considered a well-sorted sand (with shells).

The complex nature of the grain size histograms is illustrated in Fig. 9. Despite the wide range in median grain sizes, all the histograms appear to be an admixture of four different distribution peaks, at ~0.9 μm (clay), 10 μm, 50 μm (silts) and 350 μm (medium sand). The two silt size classes dominate the sandy muds, but the medium sand appears to provide a key source of variability (Fig. 9b,c). Conversely, significant silt fractions are observed within the shell-rich layer and upper shelly sand samples, as evidenced by the D10 values (Fig. 8c) as well as the histogram (Fig. 9c), but largely disappears at the deepest sample (Fig. 8c).

A shell-rich layer was commonly at the mud/sand transition where penetrated by cores. The deposits are likely allochthonous, representing a lag deposit sourced from erosion of unknown source material. The evidence for transport are twofold: (1) shells greater than 1 cm in size are commonly disarticulated and broken and (2) many of the shells (both bivalves and gastropods) have holes that penetrate the shell, which indicate that predators, such as whelks and burrowing snails, likely killed the mollusk or gastropod (Boucot, 1953).

## 4. Discussion

### 4.1 Origin of Mud Pond Accommodation Space

Deposition of the >12 m thick mud pond targeted in this study (Fig. 8b) was facilitated by the prior existence of accommodation space formed by a depression in older (presumably Pleistocene age) shelf sediments (Fig. 6b). A key observation related to the timing of the accommodation space is that sand ridges are present within the basin beneath the mud, and are built-up on the western edge of the accommodation space (Fig. 6a). This indicates that sand ridges formed in the presence of the depression, and therefore that it existed in the inner-shelf marine setting after the transgression of the shoreline across the region. Such a depression on the shelf is rare, as terrestrial depressions such as drowned river valleys are typically filled in during the transition to marine settings by estuarine muds and barrier island sands (Norfjord et al., 2006). Major river valleys, such as the Hudson Shelf Valley (Freeland et al., 1981; Fig. 1), are an exception to this characterization; presumably the accommodation space was so large that transgressive sedimentary sequences were insufficient to fill it. However, no major river valleys would have existed in our study area, which is located east of the primary drainage valleys derived from the New England rivers (McMaster and Ashraf, 1973). Instead, in the past this region was offshore of the terminus of the Laurentide glacier at Cape Cod and Martha's Vineyard (Koteff and Pessl, 1981; Uchupi et al., 2001; Balco et al., 2002). We suggest, therefore, that drainage from the ice sheet during retreat may have played a role in forming the mud pond accommodation space.

Uchupi et al. (2001) hypothesized that outburst flooding from glacially-damned lakes, formed by the retreating glacier, had a significant impact on the geomorphology of the continental shelf. We subsequently hypothesize that such an outburst flood could have eroded shelf terrain sufficiently to create the mud pond accommodation space that we observe in our survey. The former "Lake Nantucket Sound" (Uchupi et al., 1996), which formed in what is now Nantucket Sound, was the most proximal of

these lakes and therefore likeliest candidate for such an event. Emptying ~17-18 ka (Uchupi et al., 1996), this glacial lake drainage would have occurred when eustatic sea level in this region was ~100 m below present-day sea level (Wright et al., 2009), and the survey area would still have been subaerially exposed (the deepest parts of the mud base horizon are ~90 m below present-day sea level). By ~16 ka, the ice sheet had retreated to the north of Cape Cod (Uchupi et al., 2001), and glacial drainage would likely not have impacted the survey region after that time.

If the accommodation space did form subaerially, we might expect it to have been filled in by transgressive sequences, such as estuarine muds and barrier sands, as is commonly observed along coastline embayments today (Allen and Posamentier, 1993; Simms et al., 2008). However, the presence of the Hudson Shelf Valley (Freeland et al., 1981) indicates that this is not always the case; i.e., that pre-transgressive accommodation spaces can be large enough, and sediment inputs low enough, that embayments can survive the transition from subaerial to submarine settings. In addition, the pre-Holocene rapid pace of sea level rise and coastal transgression across the survey area (Wright et al., 2009) may have also inhibited infilling by transgressive sequences.

### 4.2 Transition from Sand Ridges to Mud Deposits

The stratigraphic evidence from this study indicates that, prior to the beginning of mud deposition, the seafloor in the study region was formed by oblique sand ridges that are ubiquitous on the US Atlantic continental shelf (Duane et al., 1972). As noted above, the morphological characteristics of the buried sand ridges are identical to those of modern sand ridges in the Mid Atlantic Bight, so we can assume that they formed under similar oceanographic conditions as seen today; sand ridges form initially along the shoreface and, with rising sea level and transgressing coastline, become detached from the shoreface but continue to evolve and migrate on the inner and middle shelf (Swift and Field,

1981; Goff et al., 1999; Snedden et al., 2011; Goff and Duncan, 2012). Three observations in our study indicate that the sand ridges beneath the Mud Patch were migrating under a dominantly east-directed transport regime:

(1) The acute angle of the obliquity with respect to isobaths contours is to the west (Figs. 5a, 6a). Both observational (Swift and Field, 1981) and modeling (Calvete et al., 2001) work indicate that, when forming along the shoreface, the acute angle of sand ridge orientation faces the dominant current direction.

(2) Where internal reflectors within the buried sand ridges are evident (Fig. 4), the dip direction is to the east. In addition, the largest ridges express a strong asymmetry in profile, with steeper eastern flank (Fig. 4). Both observations are consistent with a dune-like bedform with western stoss and eastern lee flanks (Ashley, 1990), and thus east-directed sediment transport.

(3) The greatest sand ridge accumulation lies on the western edge of the previously-formed accommodation space (Fig. 6a), also indicating transport from west to east that deposits suspended load when it reaches the accommodation space.

While the buried sand ridges formed and migrated under an east-directed transport regime, subsequent mud deposition appears to have been deposited under a west or southwest-directed transport regime, as evidenced by the SW progradation of the deposits (Fig. 7), and internal units that drape across the eastern shoulder of the accommodation space while onlapping on the western shoulder (Figs. 3, 4). This transport direction is consistent with the modern, west-directed shelf current directions (Twichell et al., 1981).

A central unresolved question is: why did the sedimentary environment change from sand ridge migration to mud deposition? The stratigraphic evidence of a change in primary transport direction that is coincident with this change in depositional environment appears to be a critical clue in answering this

question; it indicates a major change in physical oceanographic conditions that could have precipitated the transition.

We consider two possible explanations for the reversal of flow over the shelf relative to modern circulation over the continental shelf. The first is that wind patterns may have differed in the past. Due to the much decreased water depth during the glacial period, it would have been easier to reverse the flow with a given wind stress, such that the bottom stress would be balancing the surface wind stress. Modeling reconstructions of the atmospheric conditions during the Last Glacial Maximum suggest that the Jet Stream was much stronger than in the present day, so that the west to east wind stress may have been substantially greater than the present wind stress (Li and Battisti, 2003). This study also concludes that Jet Stream winds were more zonal in nature, and that transient storms may have been less frequent. For the modern shelf circulation in the region, an alongshelf pressure gradient also is important in driving the flow against the wind stress (Zhang et al., 2011). Both the relative increase in wind stress from the west, the shallower water depths, and the steadier zonal nature of the winds would all contribute to a flow reversal. A second possible explanation is that the Gulf Stream might have extended further north of Cape Hatteras, driving an eastward flow south of New England over the outer continental shelf. This would involve a substantial latitudinal shift in the detachment point of the Gulf Stream from the continental slope bathymetry. Evidence from formanifera distributions from this time period are not consistent with a northward shift in the separation point of the Gulf Stream (Matsumoto and Lynch-Stieglitz, 2003). Thus the preponderance of evidence would suggest that the stronger, more zonal winds combined with the much shallower depths over the continental shelf resulted in the reversal of the mean currents relative to the present day.

More details about the transition from sand ridge migration to mud deposition are provided by the core evidence (Figs. 8, 9). The shell-rich layer at the top of the sand (Fig. 8), which is commonly observed in the cores that penetrate the mud/sand boundary, could be interpreted as an erosional lag (Cattaneo

and Steel, 2003). This inference is supported by the evidence, noted earlier, that these shells have been transported rather than formed in situ. Nevertheless, the concentration of shells at the boundary can be considered as a remarkable observation, since modern sand ridges in the Mid-Atlantic Bight do not typically exhibit large quantities of shell lag at the seafloor at any water depth (Duane et al., 1972; Stubblefield and Swift, 1981; Goff et al., 2000). We therefore speculate that prevalence of the shell-rich layer at the mud/sand boundary is associated with a rapid growth in gastropod communities that may have been precipitated by the change in oceanographic conditions at that time.

Muds deposited above the mud/sand boundary include a significant sand component, whose modal grain size is identical to the sand beneath the boundary (Fig. 9). This admixture of grain sizes could be explained by the fact that, during the early stages of Mud Patch deposition, the tops of the sand ridges remained exposed in proximity. Hence, sands could have been transported laterally, perhaps by the occasional large storm, from the ridges onto nearby mud deposits. Episodicity in such a transport process could explain the presence of internal reflectors within the mud unit, and waning impact of proximal sands as the ridges became progressively buried through time could explain the reduction in reflector amplitude up-section (Figs. 3, 4). The shallowest muds are not, however, devoid of sand grain sizes, so transport of sand into the Mud Patch deposits must also be derived from distal sources.

More detailed investigation of the core-based observations will be needed to resolve issues raised above related to sourcing of muds, sands and shells in the Mud Patch. This will be the subject of a companion study led by the second author.

## 5. Conclusions

Our new stratigraphic investigation of the New England Mud Patch, using chirp acoustic reflection data and coring, provides a robust basis for analyzing the depositional history of this anomalous fine-

grained depositional environment on an otherwise sandy, non-depositional shelf. Improved understanding of the Mud Patch and the conditions that facilitate it should help us with a larger understanding of depositional processes on continental shelves. The survey focused on a deep (> 12 m) mud pond within the Mud Patch. The pond was made possible by the presence of a preexisting accommodation space, which we speculate may be attributable to earlier erosion of the subaerial shelf by glacial outwash from the Laurentide ice sheet. A marine sand layer, formed by oblique sand ridges under an east-directed transport regime, partially filled the accommodation space after shoreline transgression; sand ridges are typical of the exposed seafloor morphology across most of the US Atlantic shelf. However, subsequent mud deposition developed under a west or southwest-directed transport regime, and we hypothesize that the initiation of mud deposition was coincident with this change in hydrologic conditions. The origin of this change remains uncertain at this time, but may be related to the wind patterns and more shallow water depths over the continental shelf during the glacial periods. A significant sand fraction is observed in the Mud Patch sediments, particularly in the earlier stages of deposition. We hypothesize that the proximal tops of sand ridges, which remained exposed during the first phase of Mud Patch deposition, could have been the source of this admixture. Such sands may also account for the laminate reflections that define the stratal geometry of the Mud Patch.

**Data Availability**

Unprocessed and processed chirp reflection data used in this study are available from the Marine Geoscience Data System (http://www-udc.ig.utexas.edu/sdc/). Cores and core data are archived at the USGS Woods Hole Core Repository (https://woodshole.er.usgs.gov/operations/ia/samprepo/facilities.html).

**Acknowledgements**. The authors thank crews of the R/V *Sharp* and R/V *Endeavor* for their hard work and dedication in completing the survey mission. Goff thanks Steffen Saustrup (chirp) and Dan Duncan (coring) for their expert technical assistance during the surveys, and Shihao Liu for his tireless dedication and effort in assisting the coring effort in less-than-ideal conditions. Goff also acknowledges undergraduate research assistant Sakar Khadka for his work conducting grain size analysis on core samples. The authors also acknowledge the support of the Ocean Acoustics program at the US Navy Office of Naval Research.

**References**

Allen, G.P., and Posamentier, H.W., 1993. Sequence stratigraphy and facies model of an incised valley fill: the Gironde Estuary, France. J. Sed. Petr. 63, 378-391.

Ashley, G.M., 1990. Classification of large-scale subaqueous bedforms: A new look at an old problem. J. Sed. Petr. 60, 160-172.

Balco, G., Stone, J.O.H., Porter, S.C., and Caffee, M.W., 2002. Cosmogenic-nuclide ages for New England coastal moraines, Martha's Vineyard and Cape Cod, Massachusetts, USA. Quat. Sci. Rev. 21, 2127-2135.

Bothner, M.H., Spiker, E.C., Johnson, P.P., Rendigs, R.R., Aruscavage, P.J., 1981. Geochemical evidence for modern sediment accumulation on the continental shelf off southern New England. J. Sed. Petr. 51, 281-292.

Boucot, A.J., 1953. Live and death assemblages among fossils. Am. J. Sci. 251, 25-40.

Buczkowski, B.J., Reid, J.A., Jenkins, C.J., Reid, J.M., Williams, S.J., Flocks, J.G., 2006. usSEABED: Gulf of Mexico and Caribbean (Puerto Rico and US Virgin Islands) offshore surficial sediment data release. US Geological Survey Data Series 146, version 1.0. Online at /http://pubs.usgs.gov/ds/2006/146/S.

Butman, B., Noble, M. and Folger, D. W., 1979. Long-term observations of bottom current and bottom sediment movement on the Mid-Atlantic continental shelf. J. Geophys. Res. 84, 1187-1205.

Calvete, D., Falques, A., De Swart, H.E., and Walgreen, M., 2001. Modelling the formation of shoreface-connected sand ridges on storm-dominated inner shelves. J. Fluid Mech. 441, 169-193.

Cattaneo, A., and Steel, R.J., 2003. Transgressive deposits: a review of their variability. Earth Sci. Rev. 62, 187-228.

Chen, K., Gawarkiewicz, G., and Plueddemann, A., 2018. Atmospheric and offshore forcing of temperature variability at the shelfbreak: Observations from the OOI Pioneer Array. Oceanography 31, 72-79.

Duane, D.B., Field, M.E., Meisburger, E.P., Swift, D.J.P. and Williams, S.J., 1972. Linear shoals on the Atlantic inner continental shelf, Florida to Long Island. In D. J. P. Swift, D. B. Duane, and O. H. Pilkey (Editors), Shelf Sediment Transport: Process and Pattern, Dowden, Hutchinson and Ross, Stroudsburg, Penn., pp. 447-498.

Emery, K.O., 1965. Geology of the continental margin off eastern United States. In: Proceedings of the Symposium of the Colston Research Society 17, 1-20.

Emery, K.O., and Uchupi, E., 1972. Western North Atlantic Ocean: Topography, Rocks, Structure, Water, Live and Sediment. American Association of Petroleum Geologists, Tulsa, 532 pp.

Freeland, G.L., Stanley, D.J., Swift, D.J.P., and Lambert, D.N., 1981. The Hudson Shelf Valley: Its role in shelf sediment transport. Mar. Geol. 42, 399-427.

Garrison, L.E., and McMaster, R.L., 1966. Sediments and geomorphology of the continental shelf off southern New England. Mar. Geol. 4, 273-189.

Gawarkiewicz, G., Todd, R., Zhang, W., Partida, J., Gangopadhyay, A., Monim, M., Fratantoni, P., Malek Mercer, A., and Dent, M., 2018. The changing nature of shelfbreak exchange revealed by the OOI Pioneer Array. Oceanography 31, 60-70.

Goff, J.A., 2014. Seismic and core investigation off Panama City, Florida, reveals sand ridge influence on formation of the shoreface ravinement. Cont. Shelf Res. 88, 34-46.

Goff, J. A., and C. S. Duncan, 2012. Reexamination of sand ridges on the middle and outer New Jersey shelf based on combined analysis of multibeam bathymetry and backscatter, seafloor grab samples

and chirp seismic data. In: Li, M.Z., Sherwood, C.R. and Hill, P.R. (Eds.), Sediments, Morphology and Sedimentary Processes on Continental Shelves: Advances in technologies, research and applications, International Association of Sedimentologists, Special Publication v. 44, p 121-142.

Goff, J. A., Swift, D. J. P., Duncan, C.S., Mayer, L.A., and Hughes-Clarke, J., 1999. High resolution swath sonar investigation of sand ridge, dune and ribbon morphology in the offshore environment of the New Jersey Margin. Mar. Geol. 161, 309-339.

Goff, J.A., Olson, H.C., and Duncan, C.S., 2000. Correlation of side-scan backscatter intensity with grain-size distribution of shelf sediments, New Jersey Margin. Geo-Mar. Lett. 20, 43-49.

Goff, J. A., Austin, J.A. Jr., Gulick, S., Nordfjord, S., Christensen, B., Sommerfield, C., Olson, H., and Alexander, C., 2005. Recent and modern marine erosion on the New Jersey outer shelf. Mar. Geol. 216, 275-296.

Goff, J. A., Jenkins, D., and Calder, B., 2006. Maximum *a posteriori* resampling of noisy, spatially correlated data, Geochem. Geophys. Geosys. 7, doi:10.1029/2006GC001297.

Goff, J.A., Flood, R.D., Austin, J.A. Jr., Schwab, W.C., Christensen, B., Browne, C.M., Denny, J.F., and Baldwin, W.E., 2015. The impact of Hurricane Sandy on the shoreface and inner shelf of Fire Island, New York: Large bedform migration and limited erosion. Cont. Shelf Res. 98, 13-25.

Koteff, C., and Pessl, F., 1981. Systematic ice retreat in New England. Geologic Survey Professional Paper 1179.

Li, C., and Battisti, D., 2008. Reduced Atlantic storminess during Last Glacial Maximum: Evidence from a coupled climate model. J. Clim. 21, 3561-3579.

476 Matsumoto, K., and Lynch-Stieglitz, J., 2003. Persistence of Gulf Stream separation during the Last
477 Glacial Period: Implications for current separation theories. J. Geophys. Res. 108, 3174,
478 doi:10.1029/2001JC000861.

479 Mazzulo, J., Leschak, P., and Prusak, D., 1988. Sources and distribution of late Quaternary silt in the
480 surficial sediment of the northeastern continental shelf of the United States. Mar. Geol. 78, 241-254.

481 McMaster, R.L., and Ashraf, A., 1973. Drowned and buried valleys on the southern New England
482 continental shelf. Mar. Geol. 15, 249-268.

483 Milliman, J.D., Pilkey, O.H., and Ross, D.A., 1972. Sediments of the continental margin off the eastern
484 United States. Geol. Soc. Am. Bull. 83, 1315-1334.

485 Nordfjord, S., Goff, J. A., Austin, J. A., Jr., and Gulick, S. P. S., 2006. Seismic facies of incised valley-fills,
486 New Jersey continental shelf: Implications for erosion and preservation processes acting during late
487 Pleistocene/Holocene transgression. J.f Sed. Res. 76, 1284-1303.

488 Ross, D.A., 1970. Atlantic continental shelf and slope of the United States – Heavy minerals of the
489 continental margin from southern Nova Scotia to southern New Jersey. US Geological Survey
490 Professional Paper 529-G, 40 p.

491 Schlee, J.S., 1973. Atlantic continental shelf and slope of the United States – Sediment texture of the
492 northeastern part. US Geological Survey Professional Paper 529-L, 64 p.

493 Shearman, R. K., and Lentz, S. 2004. Observations of tidal variability on the New England shelf. J.
494 Geophys. Res. 109, C06010, doi:10.1029/2003JC001972.

495 Shepard, F.P., and Cohee, G.V., 1936. Continental shelf sediments off mid-Atlantic states. Bull. Geol.l
496 Soc. Am. 47, 441-458.

497 Simms A.R., Anderson J.B., Rodriguez A.B., Taviani, M., 2008. Mechanisms controlling environmental
498 change within an estuary: Corpus Christi Bay, Texas, USA. Geological Society of America Special
499 Papers 443, 121-146.

500 Snedden, J.W., Tillman, R.W., and Culver, S.J., 2011. Genesis and evolution of a mid-shelf, storm-built
501 sand ridge, New Jersey continental shelf, U.S.A. J. Sed. Res. 81, 534-552.

502 Stetson, H.C., 1938. The sediments of the continental shelf off the eastern coast of the United States.
503 Woods Hole Oceanographic Institution, Papers on Physical Oceanography and Meteorology 5, 5-48.

504 Stubblefield, W.L., and Swift, D.J.P., 1981. Grain size variation across sand ridges, New Jersey continental
505 shelf. Geo-Mar. Lett. 1, 45-48.

506 Swift, D J.P. and Field, M.E., 1981. Evolution of a classic sand ridge field: Maryland sector, North
507 American inner shelf. Sedimentology 28, 461-482.

508 Swift, D.J.P., Duane, D.B., and McKinney, T.F., 1973. Ridge and swale topography of the middle Atlantic
509 Bight, North America: Secular response to the Holocene hydraulic regime. Mar. Geol. 15, 227-247.

510 Swift, D.J.P., Young, R.A., Clarke, T.L., Vincent, C.E., Niedoroda, A., and Lesht, B., 1981. Sediment
511 transport in the Middle Atlantic Bight of North America: synopsis of recent observations. . In: D.J.P.
512 Swift, G.F. Oertel, R.W. Tillman and J.A. Thorne (Eds.) Shelf sand and sandstone bodies: Geometry,
513 facies and sequence stratigraphy. Special Publications of the International Association of
514 Sedimentology 5, pp. 361-383.

515 Thorne, J.A., Swift, D.J.P., 1991. Sedimentation on continental margins, VI: a regime model for
516 depositional sequences, their component systems tracts, and bounding surfaces. In: D.J.P. Swift, G.F.
517 Oertel, R.W. Tillman and J.A. Thorne (Eds.) Shelf sand and sandstone bodies: Geometry, facies and

518 sequence stratigraphy. Special Publications of the International Association of Sedimentology 5, p.
519 189-255.

520 Twichell, D.C., McClennen, C.E., and Butman, B., 1981. Morphology and processes associated with the
521 accumulation of the fine-grained deposit on the southern New England shelf. J. Sed. Petr. 51, 269-
522 280.

523 Vincent, C.E., Swift, D.J.P., and Hillard, B., 1981. Sediment transport in the New York Bight, North
524 American Atlantic shelf. Mar. Geol. 42, 369-398.

525 Uchupi, E., 1963. Sediments on the continental margin off eastern United States. US Geological Survey
526 Professional Paper 475-C, p. 132-137.

527 Uchupi, E., Giese, G.S., Aubrey, D.G., Kim, D.J., 1996. The late Quaternary Construction of Cape Cod Bay,
528 Massachusetts: a Reconsideration of the W.M. Davis Model. Geological Society of America Special
529 Paper 309, 69pp.

530 Uchupi, E., Driscoll, N., Ballard, R.D., and Bolver, S.T., 2001. Drainage of late Wisconsin glacial lakes and
531 the morphology and late quaternary stratigraphy of the New Jersey-southern New England
532 continental shelf and slope. Mar. Geol. 172, 117-145.

533 Wentworth CK. 1922. A scale of grade and class terms for clastic sediments. J. Geol. 30, 377–392.

534 Wilson, P.S., and Knobles, D. P., 2017. Overview of Seabed Characterization Experiment 2017.
535 Proceedings of the 4th Underwater Acoustics Conference and Exhibition, pp. 743–748, Ed. By J.S.
536 Papadakis. http://www.uaconferences.org/docs/Past_Proceedings/UACE2017_Proceedings.pdf.

537 Wilson, P.S., and Knobles, D. P., Overview of Seabed Characterization Experiment. Manuscript in
538 preparation for IEEE Journal of Ocean Engineering.

539 Wright, J.D., Sheridan, R.E., Miller, K.G., Uptegrove, J., Cramer, B.S., and Browning, J.V., 2009. Late
540 Pleistocene sea level on the New Jersey margin: Implications for eustasy and deep-sea temperature.
541 Glob. Planet. Change 66, 93-99.

542 Zhang, W., Gawarkiewicz, G., and McGillicuddy, D., 2011. Climatological mean circulation at the New
543 England Shelf Break. J. Phys. Oceanog. 41, 1874-1893.

544

**Figure Captions**

**Fig. 1**. Seafloor grain size map on continental shelf of the Mid-Atlantic Bight. Data are derived from the usSEABED data base (Buczkowski et al., 2006) and resampled and interpolated using the method of Goff et al., (2006) to reduce data artifacts. Depth contours, in meters, are derived from the Coastal Relief model available at the National Center for Environmental Information (https://www.ngdc.noaa.gov/mgg/coastal/crm.html). Box and expanded inset shows locations of track lines for chirp survey.

**Fig. 2**. Full-waveform chirp record from 2012 reconnaissance survey. Location shown in Fig. 1. Interior of Mud Patch is observed to be laminated, with onlap and ponding seen on undulating basal surface interpreted by Twichell et al. (1981) as relict sand ridges. Another basal reflector is noted beneath the interpreted sand ridges.

**Fig. 3**. Envelope chirp record across the full survey area, demonstrating stratigraphic character of the sediment pond targeted in the 2015 survey. Location shown in Fig. 1.

**Fig. 4**. Uninterpreted (top) and interpreted (bottom) full-waveform chirp record. Location shown in Fig. 3. The mud base (mb) reflector forms the base of the Mud Patch unit. Five interior Mud Patch reflectors (mh1-mh5) are interpreted for the purpose of investigating fill history. Beneath the mud base, we identify a sand base (sb) reflector, which often merges with the mud base at low points. Deeper still we observe another reflector, likely of Pleistocene age, dubbed “deep base” (db).

567 **Fig. 5**. (a) Structure map of the mud base (mb) horizon and (b) isopach map of the mud unit (seafloor –
568 mb). Units for both maps are in two-way travel time (twtt).

569

570 **Fig. 6**. Isopach maps for (a) the sand ridge unit (mb-sb) and (b) the presumed Pleistocene unit below
571 (sb-db). The dashed line in (b) traces the "axis of accommodation space" (see text for discussion). Units
572 for both maps are in two-way travel time (twtt).

573

574 **Fig. 7**. Isopach maps for three of the units interpreted in the mud unit: (a) mh1-mb; (b) mh3-mh2; and
575 (c) mh5-mh4. Dashed line traces the "axis of accommodation space" noted in Fig. 6b. Units for all maps
576 are in two-way travel time (twtt).

577

578 **Fig. 8**. Bottom section of vibracore VC2, which penetrates the mud/sand transition: (a) photograph of
579 split core and visual description; (b) sound speed (at 230 kHz) and gamma-ray density logs; and (c) grain
580 size distribution parameters, where D10, D50 and D90 indicate the grain sizes of the $10^{th}$, $50^{th}$ and $90^{th}$
581 percentiles, respectively, along with coarse fraction (red stars). Core location shown in Figs. 1 and 5.

582

583 **Fig. 9**. Grain size histograms for samples collected at (a) 142 cm, (b) 162 cm, and (c) 192 cm below top
584 of core VC2, shown in Fig. 8. Dashed lines identify common peaks in each of the histograms at 0.9 μm,
585 10 μm, 50 μm, and 350 μm. Grain size descriptors (clay, silt, sand) are based on Wentworth (1922)
586 classification.

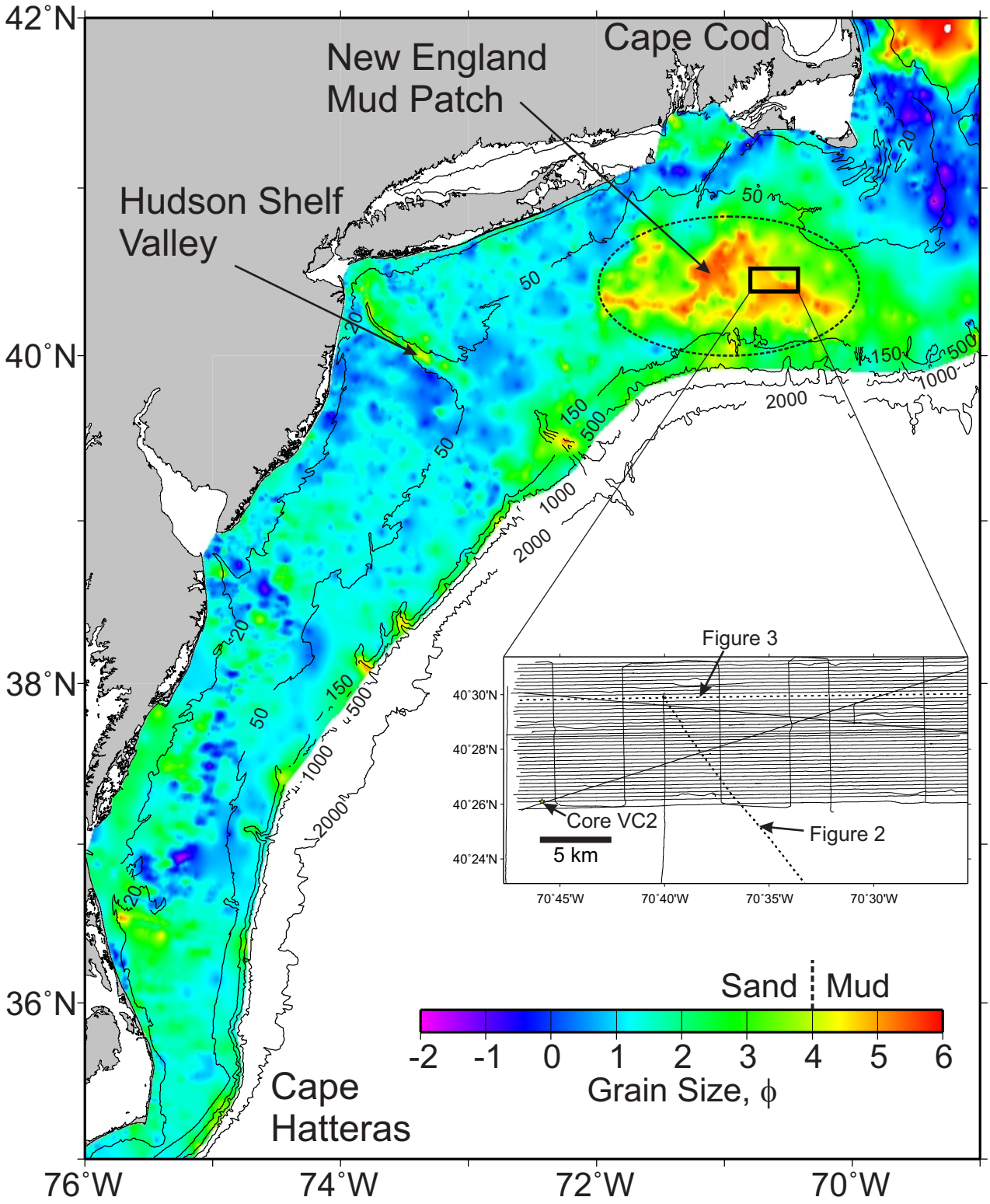
42˚N
40˚N
38˚N
36˚N
76˚W
74˚W
72˚W
70˚W
Cape Cod
New England
Mud Patch
Hudson Shelf
Valley
Cape
Hatteras
20
50
150
500
1000
2000
Figure 3
40˚30'N
40˚28'N
40˚26'N
40˚24'N
70˚45'W
70˚40'W
70˚35'W
70˚30'W
Core VC2
5 km
Figure 2
Sand
Mud
-2
-1
0
1
2
3
4
5
6
Grain Size, ϕ

Figure 1

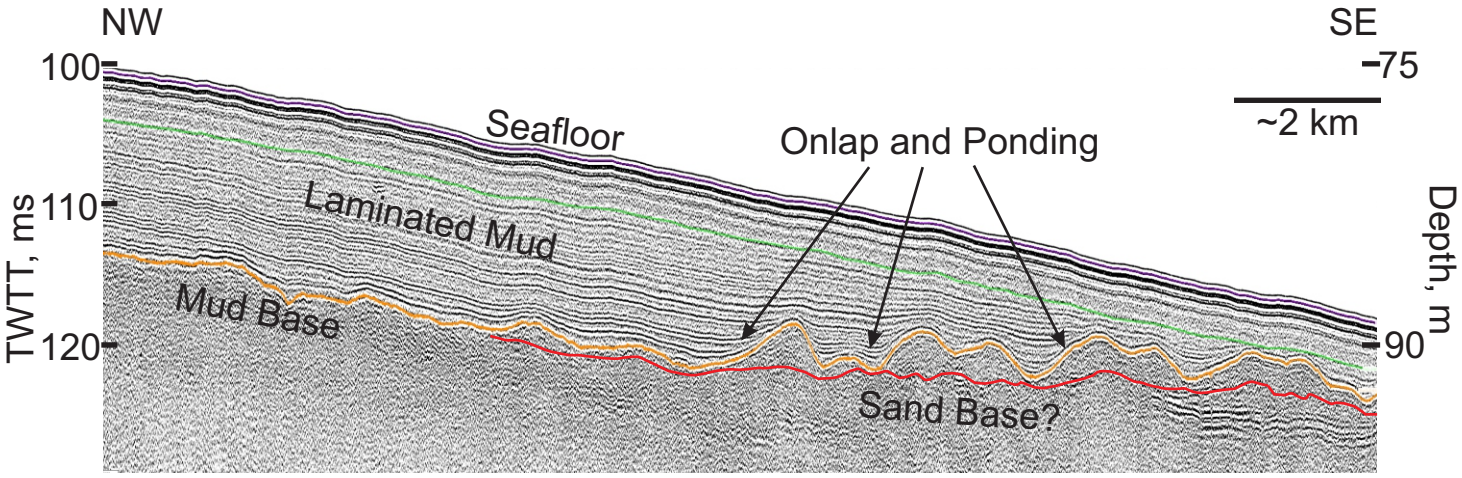
NW
SE
100
75
~2 km
Seafloor
Onlap and Ponding
Laminated Mud
110
TWTT, ms
Depth, m
Mud Base
120
90
Sand Base?

Figure 2

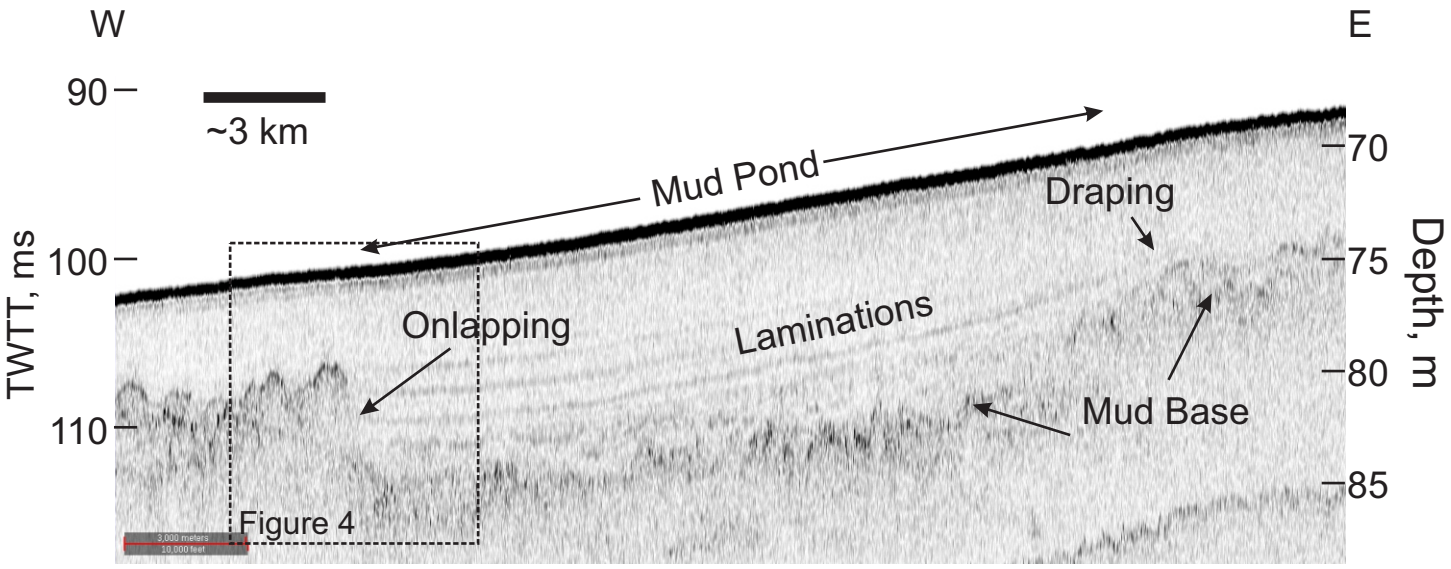
W
E
90
~3 km
Mud Pond
Draping
70
TWTT, ms
100
Onlapping
Laminations
75
Depth, m
Mud Base
110
80
85
Figure 4
3,000 meters
10,000 feet

Figure 3

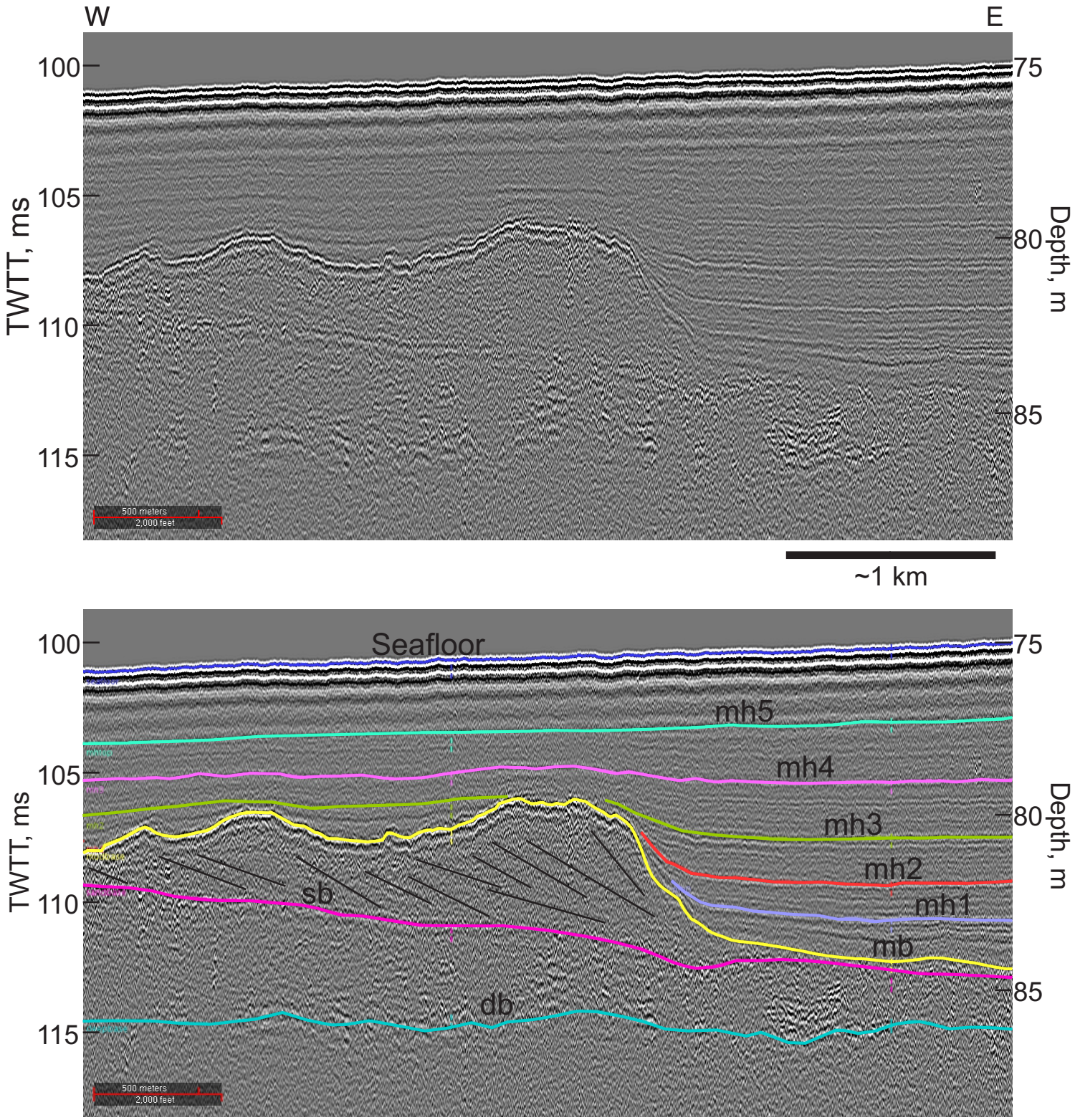
W
E
100
105
110
115
TWTT, ms
75
80
85
Depth, m
500 meters
2,000 feet
~1 km
Seafloor
mh5
mh4
mh3
mh2
mh1
mb
sb
db

Figure 4

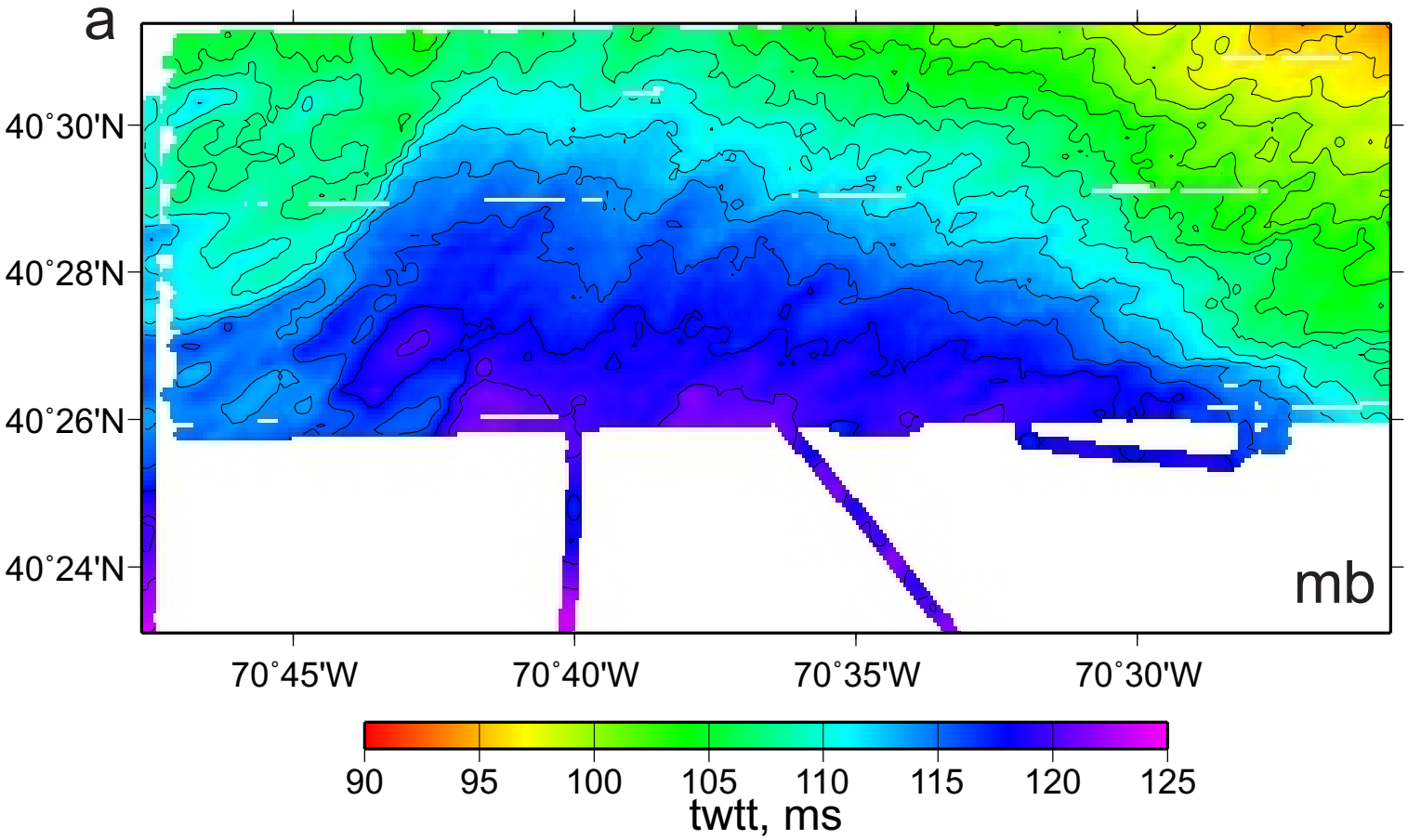
a
40˚30'N
40˚28'N
40˚26'N
40˚24'N
70˚45'W
70˚40'W
70˚35'W
70˚30'W
mb
90
95
100
105
110
115
120
125
twtt, ms

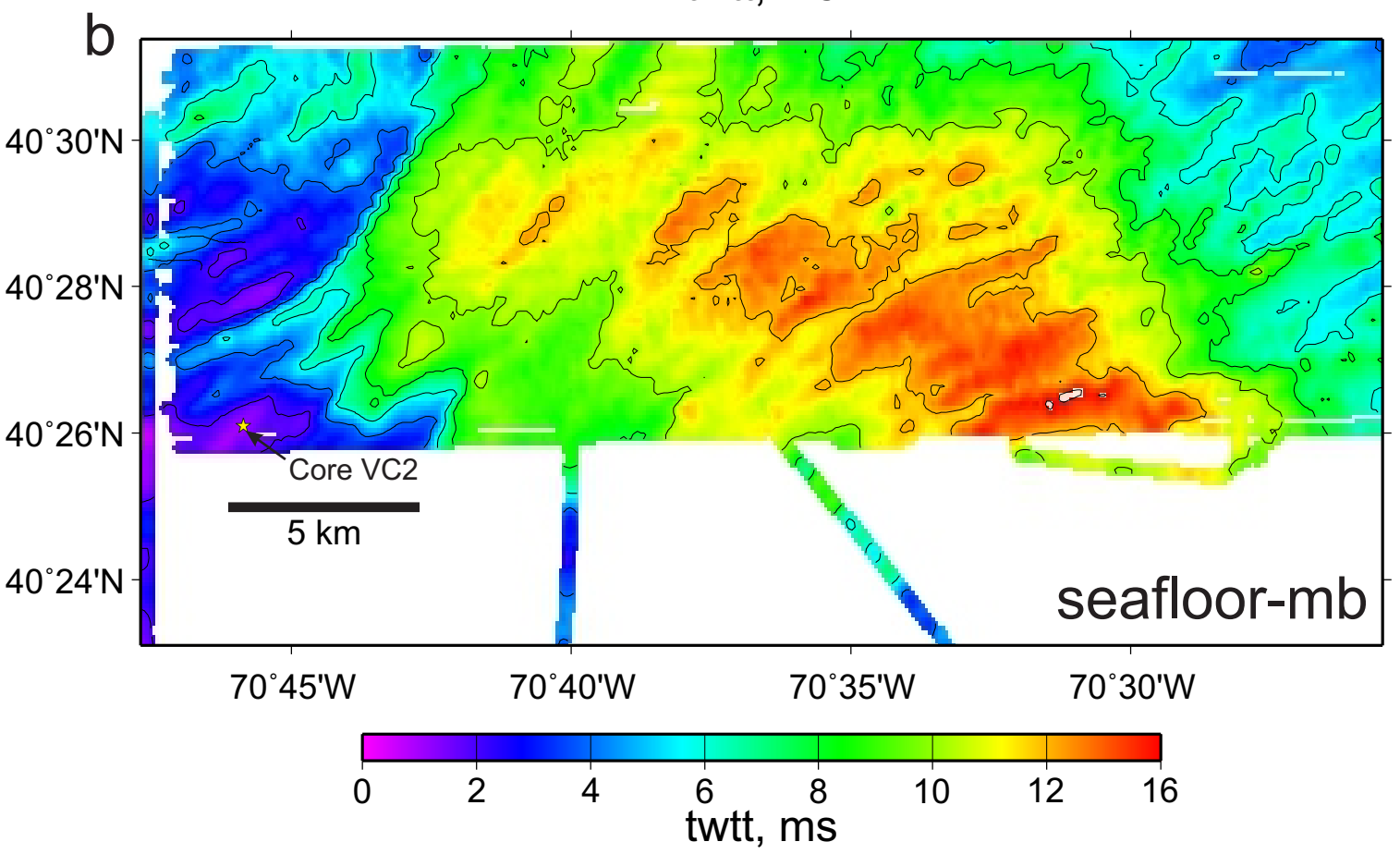
b
40˚30'N
40˚28'N
40˚26'N
40˚24'N
Core VC2
5 km
70˚45'W
70˚40'W
70˚35'W
70˚30'W
seafloor-mb
0
2
4
6
8
10
12
16
twtt, ms

Figure 5

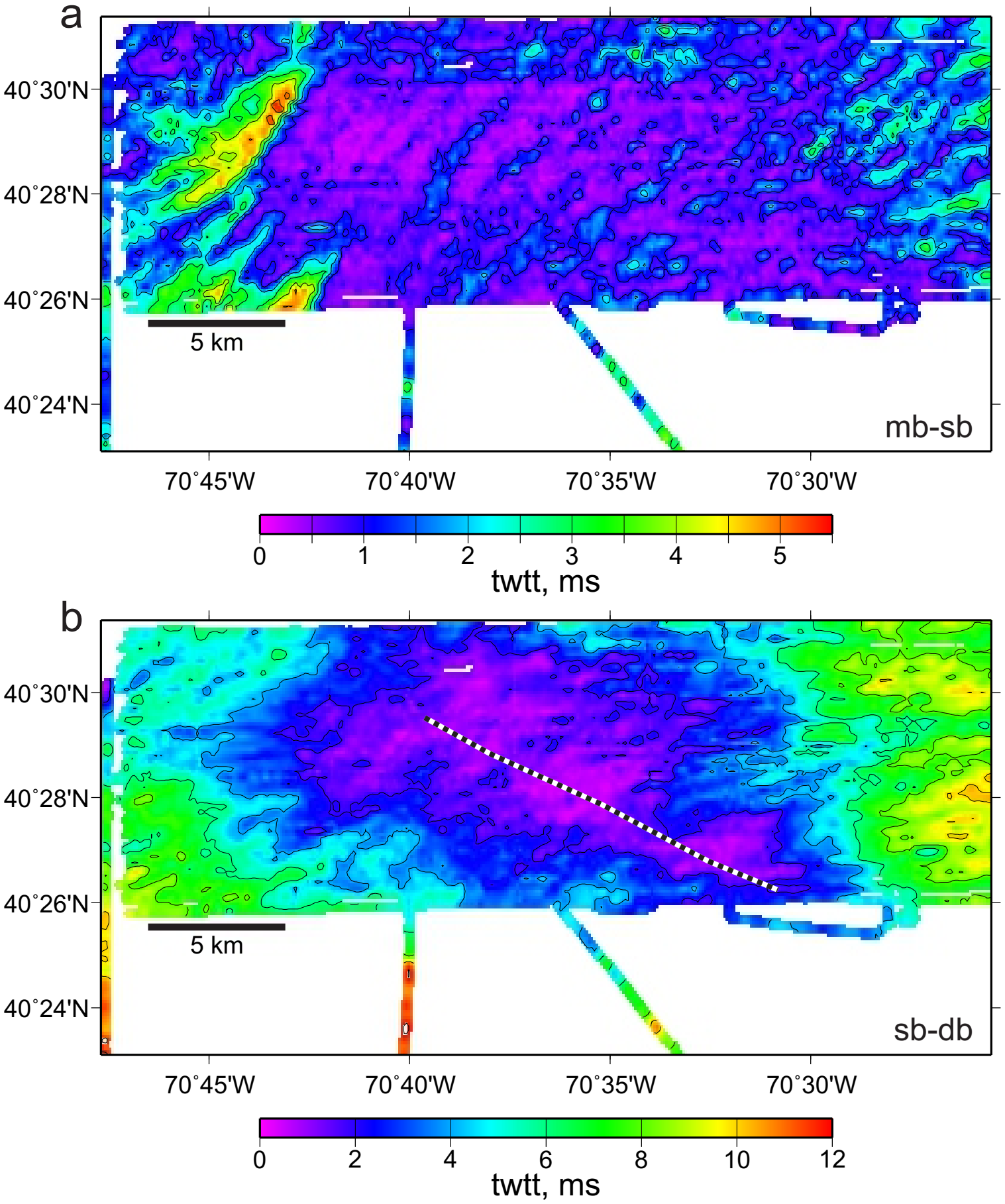
a
40˚30'N
40˚28'N
40˚26'N
40˚24'N
5 km
mb-sb
70˚45'W
70˚40'W
70˚35'W
70˚30'W
0
1
2
3
4
5
twtt, ms
b
40˚30'N
40˚28'N
40˚26'N
40˚24'N
5 km
sb-db
70˚45'W
70˚40'W
70˚35'W
70˚30'W
0
2
4
6
8
10
12
twtt, ms

Figure 6

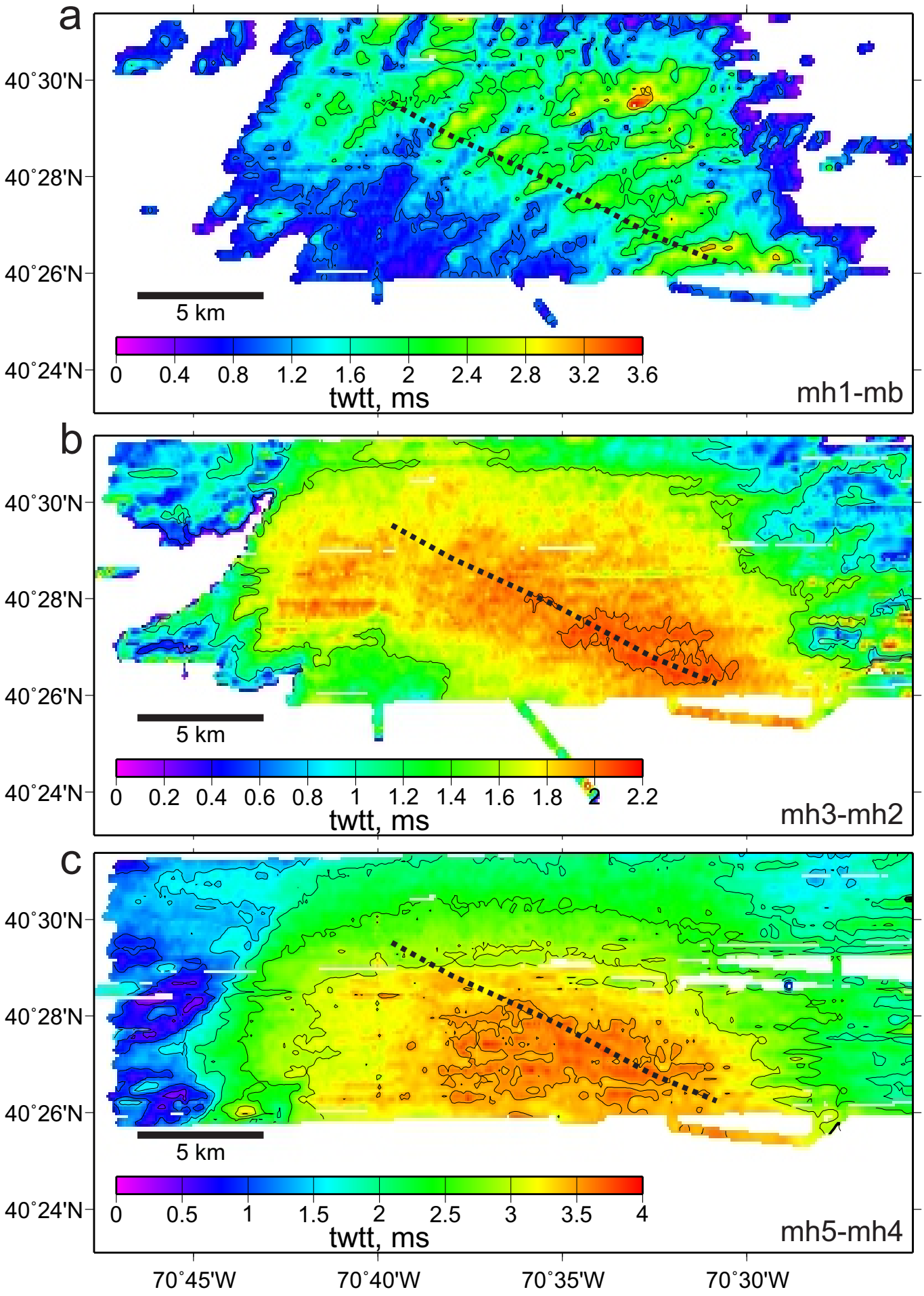
a
40°30'N
40°28'N
40°26'N
40°24'N
5 km
0 0.4 0.8 1.2 1.6 2 2.4 2.8 3.2 3.6
twtt, ms
mh1-mb
b
40°30'N
40°28'N
40°26'N
40°24'N
5 km
0 0.2 0.4 0.6 0.8 1 1.2 1.4 1.6 1.8 2 2.2
twtt, ms
mh3-mh2
c
40°30'N
40°28'N
40°26'N
40°24'N
5 km
0 0.5 1 1.5 2 2.5 3 3.5 4
twtt, ms
mh5-mh4
70°45'W
70°40'W
70°35'W
70°30'W

Figure 7

a
b
c
Depth below top of core, cm
140
150
160
170
180
190
200
Sandy Mud
Shell Mat
Shelly Sand
1600
1800
2000
2200
2400
Sound Speed, m/s
Density, kg/m3
Grain Size, ϕ
0
2
4
6
8
D90
D50
D10
0
0.1
0.2
0.3
Coarse Fraction (★)

Figure 8

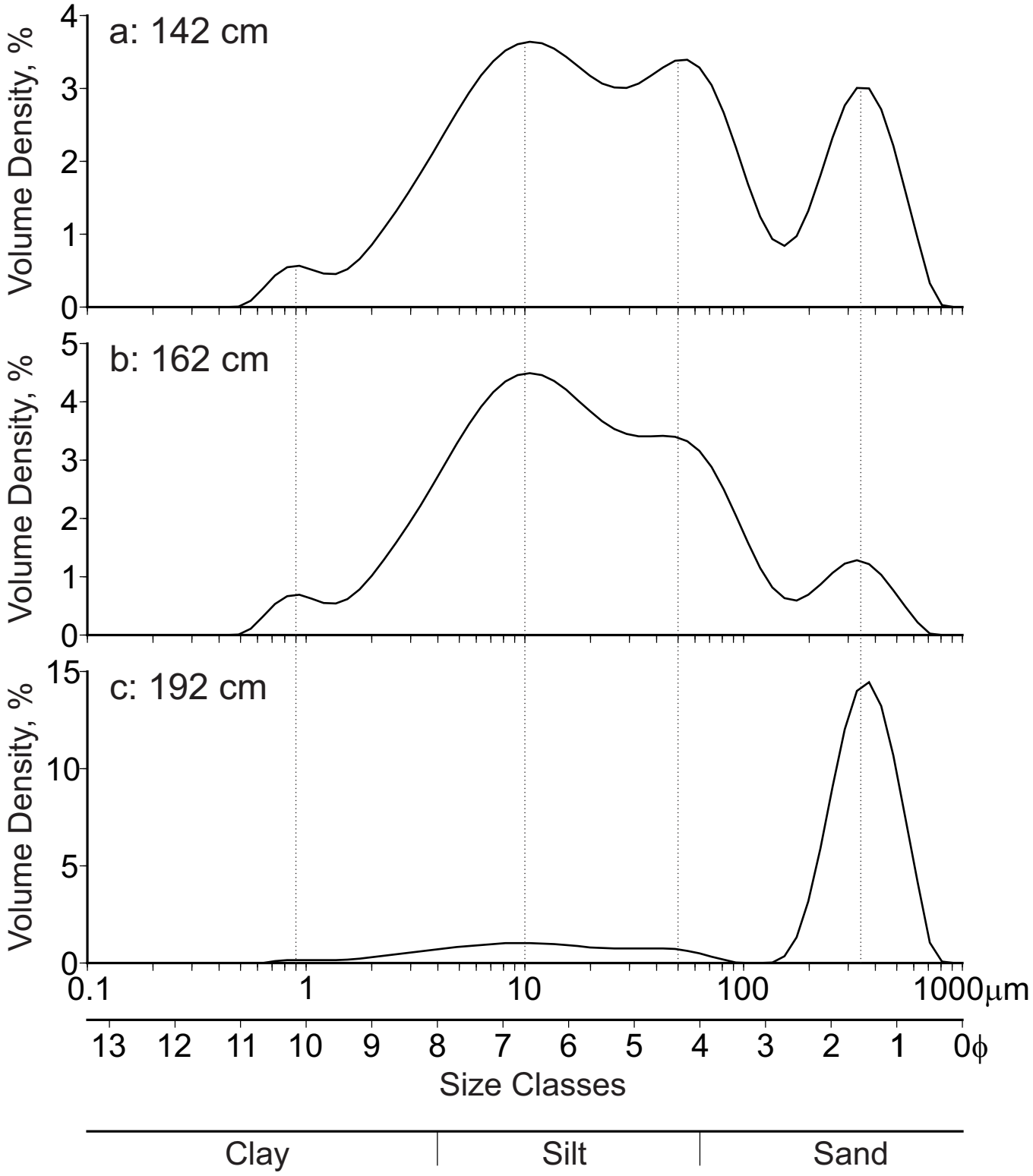
a: 142 cm
b: 162 cm
c: 192 cm
Volume Density, %
0
1
2
3
4
5
10
15
0.1
1
10
100
1000μm
13 12 11 10 9 8 7 6 5 4 3 2 1 0ϕ
Size Classes
Clay
Silt
Sand

Figure 9